Composites Part B 221 (2021) 109008

Contents lists available at ScienceDirect

Composites Part B

journal homepage: www.elsevier.com/locate/compositesb

Development and impact characterization of acrylic thermoplastic composite bicycle helmet shell with improved safety and performance

Goram Gohel [a], Somen K. Bhudolia [a,*], Shanmuga Bala Subramanyam Elisetty [a], Kah Fai Leong [a], Pierre Gerard [b]

[a] School of Mechanical and Aerospace Engineering, Nanyang Technological University, 50, Nanyang Avenue, 639798, Singapore

[b] Groupement de Recherche de Lacq, Arkema, Route Départementale 817, BP 34, 64170, Lacq, France

ARTICLE INFO

Keywords:
Thermoplastic composite
Impact
Helmets
Energy absorption
Failure

ABSTRACT

Fiber-reinforced composites are increasingly used as an outer shell of sporting helmets as an alternative to conventional thermoplastic shells like Acrylonitrile butadiene styrene (ABS), Polyurethane (PU), and polycarbonate (PC) for improved protection. The current research presents a detailed study to manufacture novel woven carbon/Elium® (WEL) thermoplastic composite helmets and investigate the details based on the impact tests following the industrial safety certification criteria (CPSC 1203 helmet certification) tests on the flat, curbstone, and the hemispherical anvils. The effect of thermoplastic Elium® resin toughened thermoplastic Elium® IM, and Epoxy resin is investigated to understand the benefits offered by the thermoplastic variants in terms of safety, energy absorption, and the impact failure mechanisms. Post-failed Carbon/Elium® thermoplastic composite shells have shown more ductile and less catastrophic damage as opposed to the Carbon/Epoxy composite shell damage. The impact damage mechanisms as observed from the in-situ high-speed camera images have shown more deformation-dominated failure mechanisms for the composite shells manufactured with Elium® and toughened Elium® resin. Carbon/Epoxy composite shells have shown lower energy absorption and the nature of the failure was more catastrophic and more cracks were noticed on the inner side of the foam which is directly attached to the human head. In case of an impact on a flat anvil, the PC shell configuration has shown a critical injury rate of 28.7% and a fatality rate of 6%. With the manufactured Carbon/Elium® composite helmets, the chances of critical and fatal injury rates are reduced to 16.7% and 3% respectively.

1. Introduction

The predominant concern regarding cycling is the accidents and the majority lead to head injuries which are common but can be very fatal [1]. More than 50% of the reported bicycle-related deaths and permanent disabilities are a result of accidents with head injuries. Furthermore, traumatic head injuries like concussions and skull fractures are found as a common cause of death [1–3]. To avoid such injuries, we must wear protective equipment i.e. helmets. It is proven that helmets play a critical and dominant role in downsizing the severity of the injury as they provide substantial protection [3,4]. With the increased daily usage, there is a higher demand for enhanced protection. Thus, there is continuous development in helmets in terms of design, material innovation, manufacturability, performance, and safety which is of utmost importance. Helmets consist of mainly two parts, an inner foam liner which is mainly the expanded polystyrene (EPS) foam, and an outer rigid shell which is usually made of conventional thermoplastics like acrylonitrile butadiene styrene (ABS), polyurethane (PU), polycarbonate (PC) or polymer composites. The primary function of inner foam is to absorb higher amount of the impact energy and to minimize the load transmitted onto the cyclist's head. However, the stiff outer shell avoids load concentration by distributing the impact of energy across a larger area. Also, the shell deformation during the impact helps in dissipating nearly 34% of the total energy [5–11]. Thus, it is very evident that further research can be done to improve the shell performance in terms of improving the energy-absorbing capability.

Composite shells are relatively more expensive than conventional thermoplastic shells but there are many associated advantages. One such major advantage is the energy-absorption. When the composite laminates are subjected to an impact, energy is not only absorbed through deformation but also through the damage mechanisms like delamination, fiber breakage, and matrix failure [7,12,13]. Also, the composite

* Corresponding author.
E-mail address: somenkum001@e.ntu.edu.sg (S.K. Bhudolia).

https://doi.org/10.1016/j.compositesb.2021.109008
Received 8 March 2021; Received in revised form 2 May 2021; Accepted 15 May 2021
Available online 25 May 2021

materials have significantly higher strength and specific stiffness as opposed to pure thermoplastic shells [14]. It specifically reduces the possibility of having brain injuries occurring due to induced accelerations [5–11]. V Kostopoulos et al. have carried out the finite element analysis on the motorcycle composite helmet [14]. Their goal was to understand the dynamic response of the helmet and the parameters that are influencing that particular response by modeling its mechanical behavior. They have used carbon fibre, Kevlar fibre, and glass fibre reinforced polyester composite system as the shell material and EPS as the liner. Their work showed that the development of the damage and the stiffness of the shell was the major influencing factors. The results were validated according to the highest acceleration observed at the center of the head-form and the peak Head injury criteria (HIC) value. Glass and carbon fibre composite shells have shown similar results but the usage of Kevlar composite shells with lower shear strength has resulted in more extensive damage through delamination and matrix cracking. They have pinpointed the demerit of using stiffer composite shell at low velocity which results in higher acceleration while in terms of energy absorbing capability the composite shells have shown significantly better properties than the conventional ABS shell at very high velocity impact. Composite shells at higher velocities absorb significant energy until the complete failure and provide more safety to the human head by transferring a lower amount of energy to the foam.

A. Cernicchi et al. studied the complicated aspects that are encountered in the virtual modeling of the protective helmet [15]. For this study, they used a helmet that is available commercially to analyze and performed the testing. The simulations for the test conditions were followed according to the ECE 22.05 standards. They emphasized particularly on the fiber-reinforced plastic shell, due to their superior performance and commented on the strain rate sensitivity and the matrix cracking phenomenon. Praveen K. Pinnoji et al. conducted a study to determine the performance of the protective helmet under impact loading [7]. The most effective failure modes of the composite shell such as the delamination and the matrix damage were investigated in detail. They found that these modes can have a vital role in terms of energy-absorbing capability. They examined the glass woven fabric/epoxy and cross-ply glass/epoxy helmet shell under impact-induced forces and concluded the benefits of the composite shells over the conventional ABS shell. The investigated fiber systems and the laminate thickness under consideration did not cause significant delamination failure and hence the energy absorption was minimal with the use of glass fiber epoxy composite shells. However composite shells have flared much better in terms of head injury criteria when compared to conventional ABS shells. Denneulin et al. studied the response of a polycarbonate and a composite plate subjected to an impact test and their energy dissipative phenomena [16]. The composite system constituted Carbon fibers with a thermoplastic matrix (Polyamide and Polyurethane). As expected, to dissipate the energy, damage mechanisms like the failure of the matrix material or fiber material, de-cohesion among the fibers, and delamination were noticed. Vishal et al. presented the research on the analysis of industrial safety helmets using composite material which has much better properties than the existing materials used in the helmets [17]. They discussed the overview of the key constructional features in a safety helmet, the advantages of composite materials in general, and the selection of appropriate composite material in their research. They have shown that the polycarbonate composite shell with 10% glass reinforcement has better mechanical strength than the conventional HDPE material. Ram et al. had worked on the design and finite element analysis of a hybrid composite motorcycle helmet [18]. The polycarbonate and polypropylene shells deformed more to the load and possess less durability and impact resistance compared to carbon fiber composite materials.

From the available literature, it is evident that numerous researches are done especially on the numerical simulations and the finite element analysis of the bicycle/motorcycle helmets. However, a very limited amount of work has presented an experimental detail on the manufacturing, testing, and understanding of the failure mechanisms of the composite helmet shells under the impact. Elium® liquid resin is a recent development by ARKEMA and suitable to use by any liquid injection techniques at room temperature [19–23]. Elium® resin can be used to impregnate fibres by using any liquid injection techniques at room temperature and results in parts having impact and fracture toughness attributes. Many studies are available in literature pertaining the fracture toughness [21,24–26], impact [22,27–31], vibration [32,33], flexure [34–36], tensile [36,37], welding [38–41] and other characteristics. Elium® resin seems to be a perfect resin owing to the above-mentioned mechanical properties, the extended plasticity behavior and it could overcome the catastrophic failure concerns with the usage of polyester and epoxy resin.

The current research presents a first detailed study to manufacture composite shells using a vacuum-assisted resin infusion process with woven carbon fiber reinforcements and novel Elium® and toughened Elium® matrix systems and carry out the helmet certification tests. Also, a detailed understanding of the failure mechanisms of the foam and the shells and the energy absorption mechanisms are established. The baseline performance comparison of novel carbon/Elium® and carbon/toughened Elium® is carried out with a conventionally used polycarbonate shell and epoxy-based composite shells by understanding the results with the help of in-situ high-speed camera investigation.

2. Materials and manufacturing

2.1. Materials

In the current research, FOE-sized and Epoxy sized 12 K 2 × 2 twill woven Carbon fibers were used for the manufacturing of thermoplastic and thermoset composite helmets respectively. The fibers were acquired from CHOMARAT, France. Elium® 150 resin and Elium® IM 150 resin was procured from Arkema, France. Elium® 150 liquid thermoplastic resin curable at room temperature, having a viscosity of 100 cP, developed by Arkema. Elium® 150 resin undergoes radical polymerization to form high molecular weight acrylic co-polymers with the addition of a benzoyl peroxide initiator at a mixture ratio of resin to hardener 100:3 at room temperature (RT) [19–23]. Elium® IM 150 is the impact modified Elium® 150 (Elium® 150 + 10 wt% of Acrylonitrile butadiene styrene copolymer (ABS)). Acrylonitrile butadiene styrene is grafted to the PMMA matrix during the polymerization of MMA and dispersed at a nano-scale [30]. To manufacture thermoset composite helmet shells, Epoxy (AM-8937 A/B) resin was used as a matrix material that was procured from Wells Advanced Materials (Shanghai) Co., Ltd. Epoxy resin cross-links with the mixture of resin and hardener at a weight ratio of 100:35. For all the different helmet configurations, the EPS inner foam of weight 112 ± 2 g was used having a density of 60 g/cm^3.

2.2. Manufacturing

A single part aluminum mould was used to manufacture the composite helmets using a Vacuum-assisted resin infusion process. The dimensions of the mould used were 421 × 345 × 143 mm^3 and the isometric view of the helmet mould is shown in Fig. 1. Preforming step was carried out with three layers (0.4 mm thick) of ±45° woven carbon fibres having dimension 450 × 420 mm^2 which were cut and placed in the mould. The preform and entire bagging setup are shown in Fig. 2a and Fig. 2b respectively. The final manufactured composite helmet shell is shown in Fig. 2c.

For the manufacturing of the thermoplastic composite shell i.e. using Elium® 150 and Elium® IM 150 resin, it was infused into the preform at room temperature (RT). After the injection was completed the inlet hose was clamped and the part was allowed to cure at RT before demoulding. Once the part was polymerised at room temperature, it was further post-cured/annealed at 60 °C in the oven for 45 min. For manufacturing of

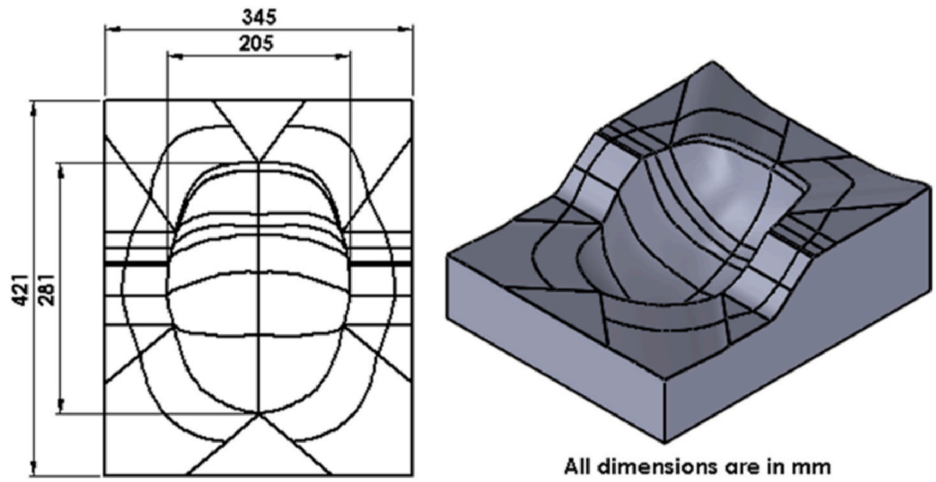

Fig. 1. CAD model and 3D isometric view of the helmet mould.

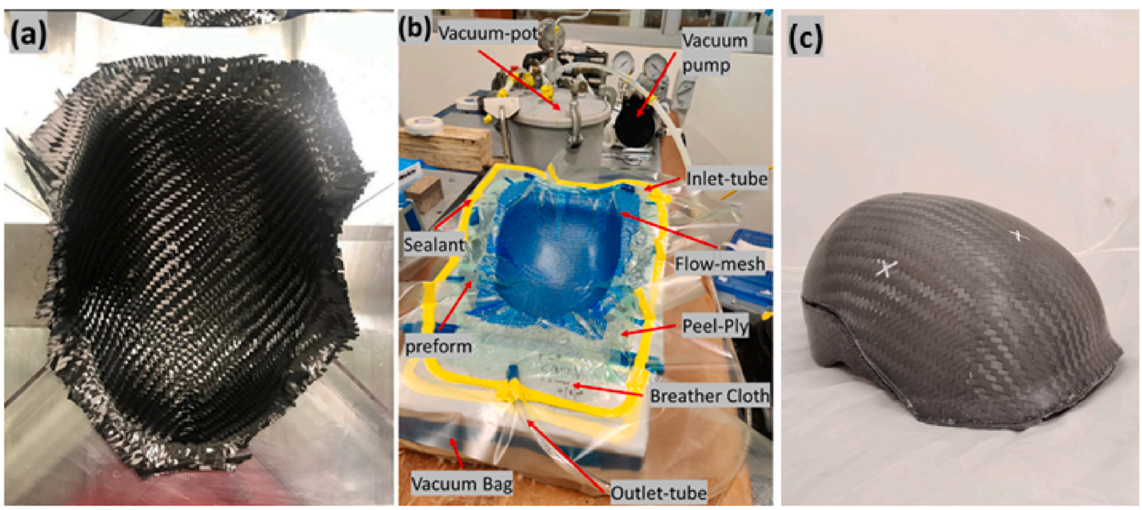

Fig. 2. (a) Preform placement into the mould (b) Bagging setup of the infusion process for the helmet shells (c) manufactured composite helmet shell.

the thermoset composite shell i.e. using epoxy resin, a heated cycle was required for infusion and curing. Before the infusion of the resin, the mould was heated to 50 °C by placing it on the hot press. Once the mould reaches 50 °C, the mixed epoxy resin was injected into the mould using a similar method as mentioned for the thermoplastic composite shell. After the resin injection, the inlet to the mould was closed and the temperature of the mould was increased to 100 °C for curing. The mould was held at this temperature for 10 min and the part was de-moulded after cooling it down to RT. The average infusion time to fill the preform for all the helmet configurations and the consolidation time to allow the resin to flow and ensure that the part is completely filled in the thickness direction are given in Table 1.

Table 1
Average infusion time for different composite shell configurations.

Composite shell configurations	Average infusion time (sec)	Consolidation time (sec)
(WovenCarbon_Elium®) Composite shell (CEL)	75	65
(WovenCarbon_Epoxy) Composite shell (CEP)	122	75
(WovenCarbon_Elium® IM) Composite shell (CEL IM)	330	265

3. Experimentation

3.1. Impact test following CPSC 1203 standard

The Impact tests were performed using the CADEX impact machine (ISO 9001–2015 certified) (refer to Fig. 3). The impact parameters such as peak acceleration, peak force, impact velocity, contact time, and Head Injury Criteria (HIC) values were obtained from the data acquisition system. HIC is calculated by the data acquisition system using the following equation (3.1) [9,44].

$$HIC = (t_2 - t_1)\cdot\left[\frac{1}{t_2 - t_1}\int_{t_1}^{t_2} a(t)dt\right]^{2.5} \tag{3.1}$$

where.

HIC Head Injury Criterion [−], Acceleration [m/s^2], t_1 Initial time of the critical period [s], t_2 Final time of the critical period [s].

The velocity during the impact was measured by the flag mounted on the impactor which operates simultaneously with the velocity detecting assembly attached (refer Fig. 3) following the CPSC 1203 standard. The values of velocity, displacement, and absorbed energy quantities were extracted by carrying the sequential integration of transient force obtained from the data acquisition system [22,42]. The test was performed

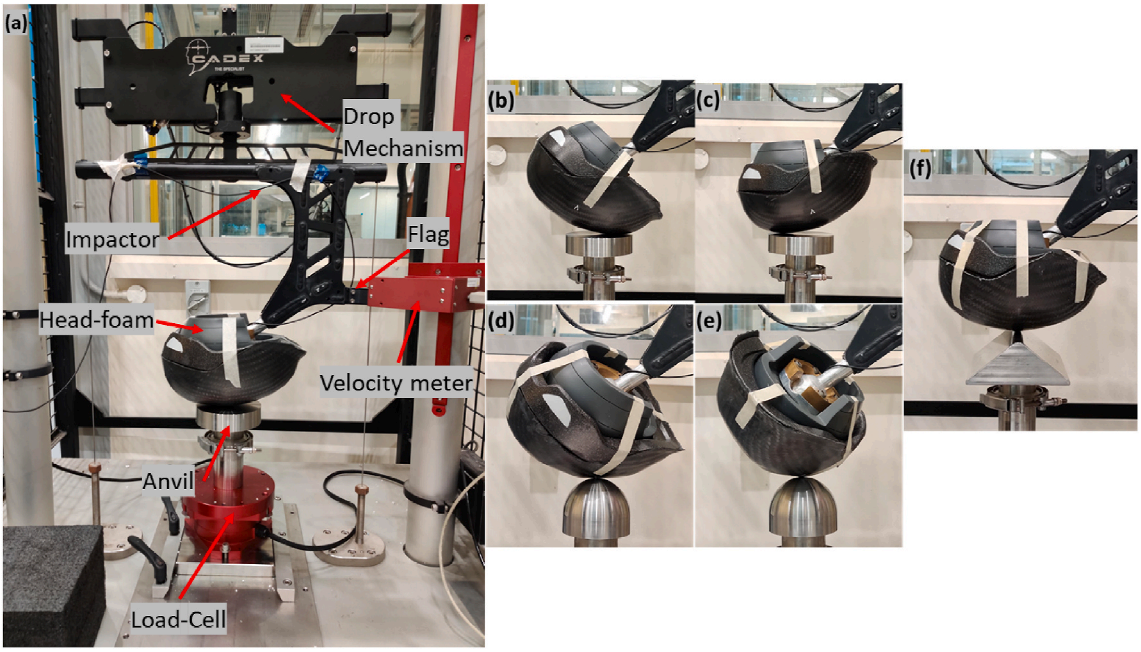

Fig. 3. (a) Experimental setup using CADEX impactor (b,c) Flat anvil impact sites 1 & 2 (d,e) Hemispherical anvil impact sites 1 &2 (f) Curbstone anvil impact site.

following the CPSC 1203 standard, using a head-form along with an impactor weighing 5 kg with flat, hemispherical, and curbstone anvils. According to the CPSC 1203 standard, the testing should be performed on 2 helmets. Helmet 1 was impacted at 4 different locations. Two out of the four impacts were performed on the flat anvil (refer Fig. 3b,c), while the other two were tested on the hemispherical anvil (refer Fig. 3d,e). It should be noted that the center of all 4 impact sites was kept at least 120 mm apart when measured on the surface of the helmet, from any prior impact location. Helmet 2 was impacted at a single site, on the curbstone anvil (refer Fig. 3f). The test schedule summary is given in Table 2.

3.2. Cut-out samples and high-speed camera (HSC) test setup

Cut-outs of the helmet shell, as well as the inner foam, were cut from the full helmet to a coupon size of 100 mm × 100 mm using the water jet cutter and hot wire cutter respectively. Cut-outs were made to observe and understand the failure mechanisms of the shells and the foam. The coupons were also tested according to the CPSC 1203 standard specification on a curbstone anvil (refer Fig. 4). To understand the damage mechanism and to better analyze the failure of the coupons, the impact event was captured using the Phantom Camera Control (version 3.4) software (refer Fig. 4) using a frame rate of 1000 fps. Then, using the individual frames at certain time intervals, the damage analysis was carried out. Samples from each helmet category were selected for HSC testing.

Table 2
Test schedule of CPSC 1203 safety standard for a Bicycle helmet.

Test standard	Helmet no.	Type of anvil/no. of impacts	Certification criteria
CPSC 1203 safety standard for Bicycle Helmets	Helmet 1	(a) Flat/Impact 1 (b) Flat/Impact 2 (120 mm apart)	<300 G at 6.2 m/s
		(c) Hemispherical/ Impact 1 (120 mm apart) (d) Hemispherical/ Impact 2 (120 mm apart)	<300 G at 4.8 m/s
	Helmet 2	(e) Curbstone/Impact 1	<300 G at 4.8 m/s

4. Results and discussion

The details of the impact dynamics of the helmet were studied by understanding the load, time, and energy characteristics of the thermoset and thermoplastic composites helmets. The failure mechanism of the helmets was studied in detail by carrying out high-speed camera analysis and observing the failure modes on the outside and inside of both the shells and foam of the helmet. Table 3 shows the nomenclature used for the helmet configurations. The impacted energy on the helmet is absorbed via different mechanisms including elastic and plastic deformation of foam/shell or by damage/failure of the specimen in the form of a dent, crack formation, delamination of the composite shell, compression of the foam, perforation, friction, and many others [22,43].

The major criteria to certify the sporting helmets using CPSC 1203 standard is based on peak acceleration. Another factor termed as Head Injury Criteria (HIC) factor takes into account not only the peak acceleration causing a certain injury, but also the duration of the impact [44–46]. The impact results were compared among the different resin systems by studying the load-time curve, energy absorbed by each configuration, HIC value, peak acceleration, and also the damage analysis which was carried out by observing the crack and damage in both shell and foam. The failure mechanisms are also understood through in-situ high-speed camera observations. It should be noted that for each configuration, two samples were tested for each anvil. It should be noted that for each configuration, two samples were tested. Later, the graph which is the best representative curve within the same configuration and is closer to the average value is shown for the analysis in the subsequent sections for impact with different anvils.

4.1. Impact of carbon reinforcement helmet: curbstone anvil

a. Testing and data analysis

Fig. 5 shows the impact analysis of all the configurations on the curbstone anvil, where Fig. 5a represents the load-time curve, Fig. 5b represents the energy absorption curve and Fig. 5c shows the peak acceleration of all the configurations. Table 4 shows the obtained, analyzed, and calculated values for all the configurations impacted on the curbstone anvil. The energy at a certain point can be calculated as an

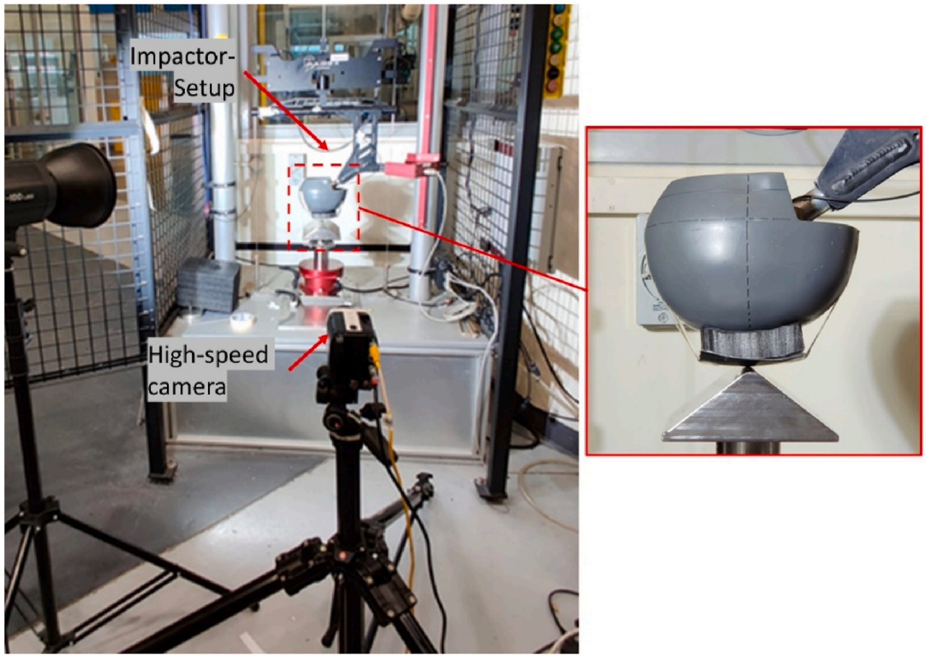

Fig. 4. PCC high-speed camera setup with 100 mm × 100 mm helmet cut-out sample.

Table 3
Helmet configurations and their nomenclature used in the current project.

Helmet configurations	The nomenclature used in the manuscript
(WovenCarbon_Elium®) Composite shell/EPS foam	CEL/EPS
(WovenCarbon _Epoxy) Composite shell/EPS foam	CEP/EPS
(WovenCarbon _Elium® IM) Composite shell/ EPS foam	CEL IM/EPS
Polycarbonate shell/EPS foam (Reference)	PC/EPS

area under the load-displacement curve. In the energy curve, the maximum value signifies the impact energy of the helmet and the last data point on the curve represents the total energy absorbed by the helmet.

From the load-time graph (refer Fig. 5a), it can be observed that the peak load of CEP/EPS configuration is 10% and 8.2% higher compared to the CEL/EPS and CEL IM/EPS composite shell configurations respectively. Also, the peak acceleration value is proportionally higher for the CEP/EPS configuration, 9.5%, and 8% compared to the CEL/EPS and CEL IM/EPS configuration respectively. Whereas, the reference helmet i.e PC/EPS helmet shown a comparatively higher peak load compared to all the composite configurations. The similarity is reflected in the peak acceleration where the PC/EPS helmet shows a 15% higher value as compared to the CEL/EPS composite helmet. When the contact time of all the configurations is compared, it can again be observed that CEL IM/EPS shows the best result among all the configurations with a maximum contact time of 11.67 ms. The increase in contact time for toughened IM Elium® is due to the additional ductility induced in the Elium® resin with ABS [28,30,47]. The toughened Elium® exhibit better crack resistance, have higher damage resistance, and have significantly higher molecular weight with very high toughness [35,48–53]. These properties lead to extended plasticity behavior in the case of toughened thermoplastic Elium® resin and must have resulted in higher contact time during the impact event. PC/EPS configuration shows the least contact time which is 21% and 16.5% lower than the CEL IM/EPS and CEL/EPS configuration respectively. Also, CEP/EPS configuration shows a 15% lower contact time compared to CEL/EPS configuration. From Table 4, it can be observed that the %total absorbed energy is almost similar for all the composite shell configurations. For reference PC/EPS helmet, the amount of % of absorbed energy is slightly higher. But, herein, the maximum load is transferred to the foam and as a result, maximum energy absorption is through the severe damage in the foam which is not an ideal condition. For PC/EPS configuration, 82.8% of the energy is absorbed by the foam whereas, in the case of the composite helmet, CEL/EPS, CEL IM/EPS, and CEP/EPS configurations have shown 12.8%, 33.3%, and 21.1% absorbed energies. As HIC takes into account both the peak acceleration and the contact time, it can be observed that the HIC of the CEP/EPS configuration is highest among the composite shell configurations (refer Table 4). This also directly relates to the value of the peak acceleration which was higher for CEP/EPS configuration and the contact time which was least among composite shell configurations. This resulted in the higher value of HIC for CEP/EPS configuration due to the catastrophic failure of the epoxy shell owing to the thermoset brittle behavior.

b. High-speed camera (HSC) analysis

As explained earlier, to better understand the failure of the shell and the foam, the HSC analysis was carried out on the coupon level for all the configurations on the curb-stone anvil. Fig. 6 shows the snapshots of the impact event recorded by a high-speed camera during an impact on the curb-stone anvil for all the configurations where the first image represents the start of the impact event, the second image represents the first load drop which corresponds to the crack formation in the foam in the load-time curve. 3rd image represents the full compression stage i.e. the peak load condition of the impact event where the foam is fully compressed. These events can be directly correlated with the load curve and match with the event timings with respect to HSC testing failure events. Fig. 7a shows an example of a load-time curve depicting different instances of failure in the foam and the shell for composite and the polycarbonate shell configuration. Also, Fig. 7b and c show the load-displacement curve and the energy absorption contours for the PC/EPS and CEL/EPS configurations. The majority of the energy for PC/EPS configuration is absorbed by foam (49.9 J) as opposed to only 9 J energy absorbed by the foam for CEL/EPS configuration and the remaining 42 J energy is absorbed by the CEL composite shell through failure and

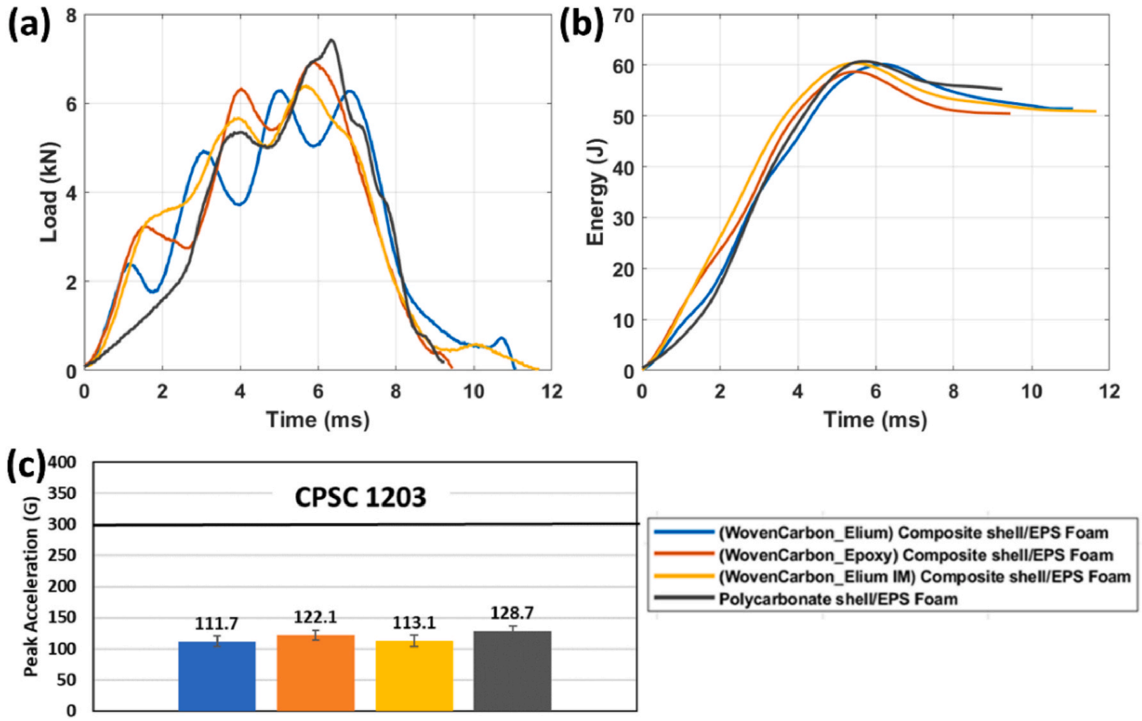

Fig. 5. (a) Load-time curve (b) Energy-time curve and (c) Peak acceleration for all the configurations impacted on the curb-stone anvil.

Table 4
Calculated and Analyzed values for all helmet configurations impacted on the curb-stone anvil.

Helmet configuration	CEL/EPS	CEP/EPS	CEL IM/EPS	PC/EPS
Shell weight (g)	155	153.7	155	116
Helmet weight (g)	262.5	265	265.2	230
Peak Acceleration (G)	111.7 ± 8.6	122.1 ± 7.98	113.1 ± 8.86	128.7 ± 7.9
Peak Load (kN)	6.29 ± 0.34	6.92 ± 0.44	6.39 ± 0.23	7.42 ± 0.36
E_{im}(J)	60.12	58.67	60.33	60.96
E_{ab}(J)	51.39	50.45	50.9	55.25
Absorbed energy at the end of impact event (%)	83.01	83.71	81.47	89.67
$t_{contact}$ (ms)	11.06	9.45	11.67	9.24
HIC	413	446	414	500
Major energy absorbed energy by shell (%)	70.21	50.39	60.34	6.87
Major energy absorbed energy by foam (%)	12.8	33.32	21.13	82.8

deformation.

For CEP/EPS helmet (refer to Fig. 6b2), it can be observed that there is a crack formation at around 2.7 ms, and a corresponding load drop observed in Fig. 5a. Further, there is a crack propagation during the later event which can be observed from Fig. 6b3. A similar phenomenon can be also observed for PC/EPS configuration (Fig. 6(b1-b3)) where the crack formation and propagation in the foam can be observed. For, CEL/EPS and CEL IM/EPS configurations, no clear/severe crack formation was observed in the foam which is directly related to the damage images of both configurations as shown in Fig. 9a,c. After the completion of the impact event, for CEL/EPS and CEP/EPS configurations, it can be seen that the shell has a brittle failure in the CEP/EPS configurations (refer to Fig. 8b) whereas permanent deformation in the case of CEL shell (refer to Fig. 8a) is noticed. At the end of the impact event, the CEL shell is significantly deformed (Fig. 6a3) and from Fig. 8a, the failure of the shell is evident with cracks with ductile failure [22,29,36,43] as opposed to the catastrophic failure as in the case of CEP shell. Thus, from the HSC analysis, it can be observed that composite shell performs better in terms of the severity of the crack through the thickness direction and the compression compared to PC/EPS helmet. Also, considering the crack formation and failure mechanisms, CEL shell configuration showed benefits over the CEP/EPS helmet.

a. Damage analysis

Fig. 9 shows the post-failure images of all the configurations impacted on the curb-stone anvil. From the load-time curve and maximum absorbed energy data (refer to Fig. 5a and Table 4), it can be observed that for PC/EPS helmet takes the maximum amount of load and the maximum amount of the energy is also absorbed by the foam. This maximum absorption of energy is due to the failure of the foam and is not ideal for human head safety. This can be directly co-related by the failure images of the foam of the reference helmet as shown in Fig. 9d.

CL represents the crack length and CW represents the crack wide opening which infers to the severity of the crack. PC/EPS configuration shows a severe crack on the inner side of the foam of crack length 35 mm and a width of 1 mm. Also, when the outer side of the foam is observed, there is a severe dent with compression of 7 mm and the spread is 135 mm. On the contrary, it is observed in the case of the composite shells. the first load drop is very early, so there are crack formation and a slight failure of the foam. Later most of the load is carried by the composite shell and energy is absorbed majorly by the shell failure and there is minimal damage in the foam (refer to Fig. 9a-c). The above explanation can be directly verified from the failure images of all the configurations shown in Fig. 9. Fig. 9 shows the post impacted failure images of the shell and the foam of all the configurations impacted on the curb-stone anvil. From the failure images, it can be observed that the failure in the CEL/EPS and CEL IM/EPS helmet configurations are almost similar. There is no significant propagation of the crack on the inner side of the shell and the foam. Whereas, in CEP/EPS helmet there is huge damage in the outer composite shell with crack length (CL) 110 mm which is further propagated into the inner side of the shell with a CL of 35 mm.

More damage in the CEP/EPS shell is due to the brittle nature of the

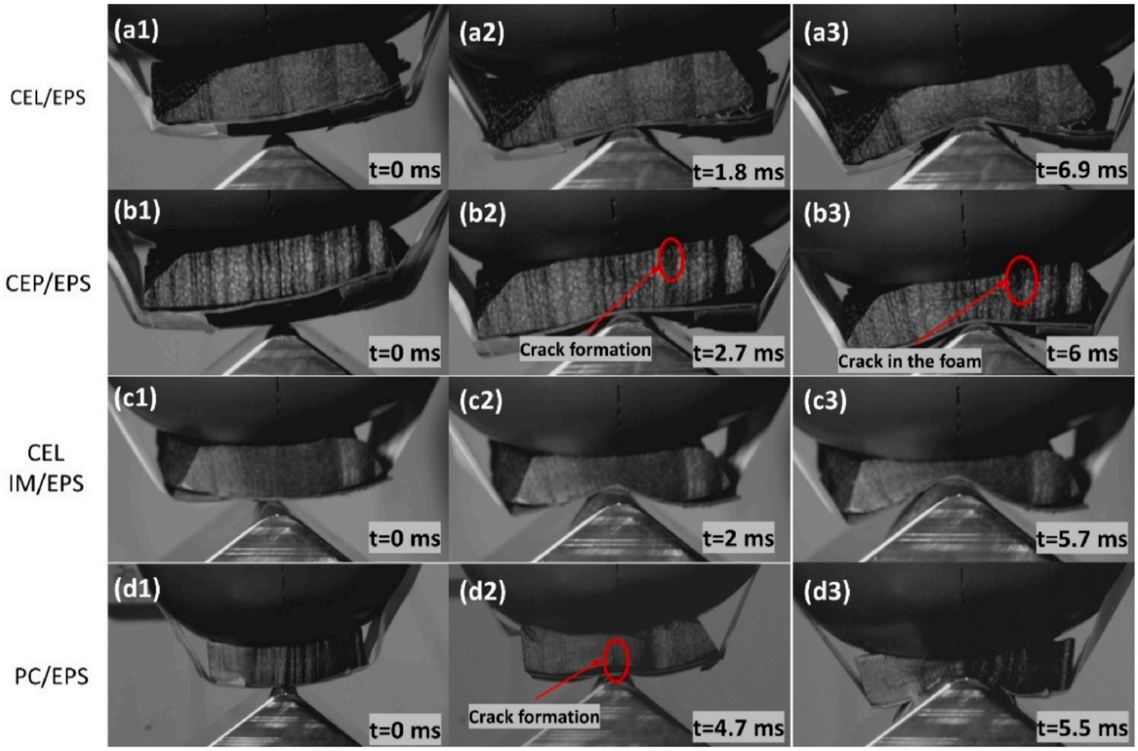

Fig. 6. High speed camera impacted events captures for all the helmet configurations (a1-a3) CEL/EPS (b1-b3) CEP/EPS (c1-c3) CEL IM/EPS (d1-d3) PC/EPS.

Epoxy resin which leads to the catastrophic failure of the shell. As a result, there is also a huge compression of the outer foam of depth 6 mm, and a massive is crack formed on the inner side of the foam with CL of 40 mm. The higher failure and the crack propagation to the foam in CEP/EPS are directly related to the shell failure mechanism, where the energy is absorbed by the catastrophic failure of the shell owing to the thermoset behavior whereas there is more permanent deformation in the CEL/EPS owing to the viscoelastic and ductile nature of acrylic thermoplastic Elium® resin [22,29,36,43].

4.2. Impact of carbon reinforcement helmet: flat anvil

a. Testing and data analysis

The impact testing on the flat anvil was carried out at 2 impact sites separated by 120 mm apart with an impact velocity of 6.2 m/s. For all the helmet configurations impacted on the flat anvil, there was no significant crack propagation in the foam or the shell on the first impact which was significant to influence the damage propagation on the 2nd impact site which is impacted at 120 mm apart. Fig. 10a represents the load-time and Fig. 10b represents the energy-time graphs of the first impact for all the helmet configurations. The analyzed and recorded values of both 1st and 2nd impacts for all the helmet configurations are represented in Table 3.

In Fig. 10a, many load drops can be observed. The first load drop directly corresponds to the crack formation or the internal damage in the foam. It also signifies the amount of load taken by the foam and the corresponding time in the Energy-time curve shows the energy absorbed by the foam. Similarly, the load drops just before the peak load has reached during the impact event is representative of the internal damage or the crack formation in the shell where the majority of the load is taken and energy is absorbed by the shell. The remaining energy is attributed to the energy absorption by the full compression of the foam.

Table 5 shows the (%) major absorb energy by the failure and/or deformation in the shell and the foam. From Fig. 10a, it can be depicted that the peak load for all the helmet configurations is very similar. Considering the contact time, it can be observed that Elium® 150 composite and Elium® IM composite helmet showed longer contact time as compared to the Epoxy composite helmet. The increase in contact time is directly related to safety, the higher the contact time, the safer is the impact event for the helmet application. From Fig. 10c, it can be observed that all the helmet configurations pass the CPSC 1203 criteria of a maximum of 300 G. For peak acceleration, lower is better. CEP/EPS configuration shows an 8.08% and 5% higher peak acceleration compared to CEL/EPS and CEL IM/EPS helmet configurations. But when compared to the PC/EPS configuration, the peak acceleration is about 9.2% higher compared to the CEL/EPS configuration. Similarly, for the energy absorption (Fig. 10b and Table 5), it can be observed that the total % absorbed energy for CEL/EPS configuration (86.405 J) at the end of the impact event is much higher than the energy absorbed by CEP/EPS (69.95 J).

Considering the energy absorption phenomenon, the benefit of the thermoplastic Elium® resin can be clearly observed. The failure in the CEL/EPS configuration is the combination of damage as well as the permanent deformation due to the ductile nature and the extended plasticity behavior of acrylic thermoplastic Elium® resin [22,29,36,43]. For CEP/EPS configuration, the energy is absorbed by the catastrophic failure of the shell due to the brittle behavior of the epoxy resin. In the PC/EPS configuration, the % absorbed energy is almost similar to the CEP/EPS configuration barring that the failure in the former is more significant. For PC/EPS configuration, the majority of the load and energy absorption is taken by the foam and the shell acts as supporting material. As seen from Table 5, the % major absorbed energy by foam in the PC/EPS configuration is 75.39% which results in the higher failure and deformation of the foam. This is not an ideal condition as the foam is in direct contact with the human head. As opposed to the PC/EPS configuration, all the composite shell configurations have shown higher energy absorption by shell compared to the foam. The higher energy absorption characteristics of the shell are preferred as less amount of load will be transferred to the foam. Another important factor is the HIC, which indicates the severity of the damage considering the acceleration along with accounting for the contact time. From Table 5, it can be

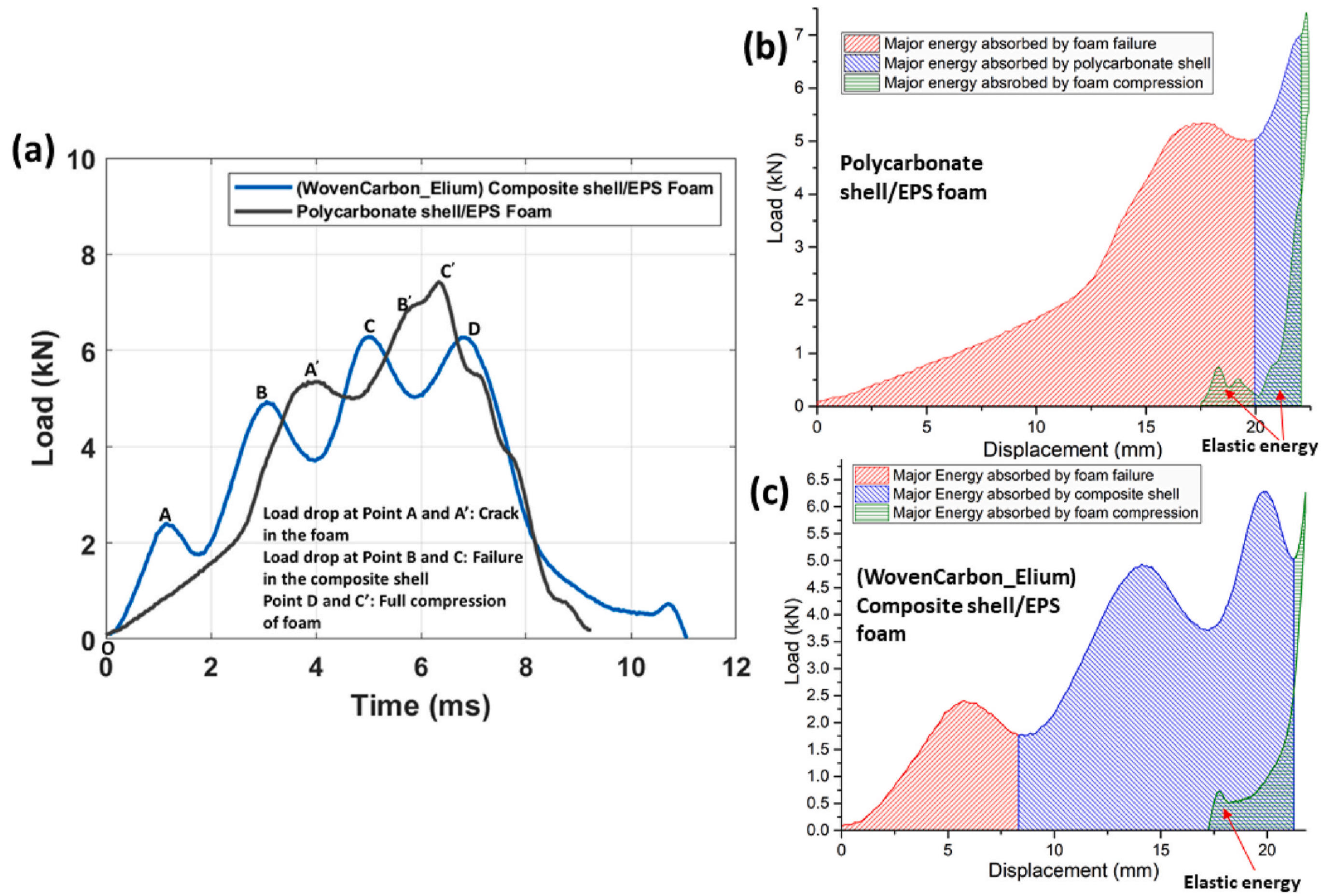

Fig. 7. (a) Different instances of failure in the foam and the shell in load vs time curve (b,c) Load vs displacement curve and respective energy contours for foam and shell for PC/EPS configuration and CEL/EPS configuration.

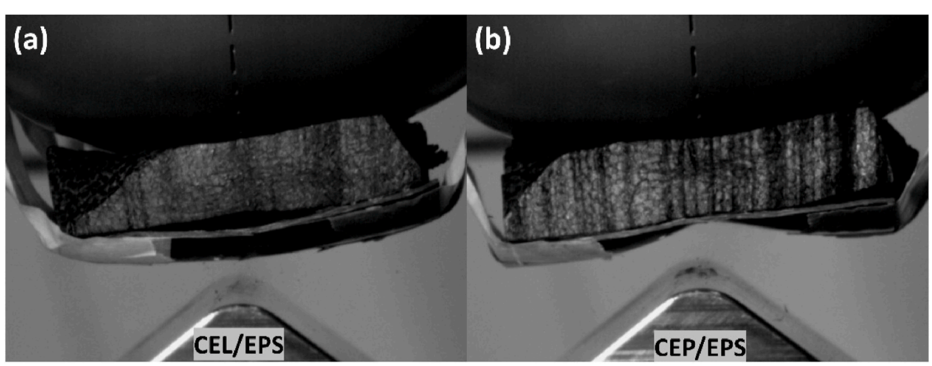

Fig. 8. High-speed camera capture after the impact event for (a) CEL/EPS (b) CEP/EPS.

observed that all composite helmet configurations are below 1500 HIC value. CEL IM/EPS configuration showed the least value which is 8% lower than the CEP/EPS configuration. Below the 1500 range, the critical injury is below 20% and the fatality rate is around 3% [46]. But when compared to PC/EPS configuration the HIC is 1592 which corresponds to the critical injury rate of 30% and the fatality rate of 6%.

b. Damage analysis

After the impact event, the damages for all the helmet configurations were analyzed by observing the failure of both the shell and the foam of the helmet on both the inner and outer sides as shown in Fig. 11. From Fig. 11a,c, it can be observed that CEL/EPS and CEL IM/EPS helmet configurations have shown similar failure in the shell and cracks in the foam. CEL IM/EPS configuration shows slightly less crack formation on the inner side of the foam where the crack length (CL = 40 mm) is much lower compared to crack length (CL = 70 mm) for CEL/EPS configuration. As observed from Fig. 11b, in CEP/EPS configuration, there is a more concentrated and catastrophic failure in the shell due to the brittle behavior of the Epoxy resin. The crack formed in the foam is much severe with a crack length of 65 mm and significantly higher crack width of 1 mm whereas, in CEL/EPS and CEL IM/EPS configurations (Fig. 11a, c) more spreaded failure with multiple cracks on the shell can be observed due to the ductile behavior of thermoplastic Elium® resin [22,

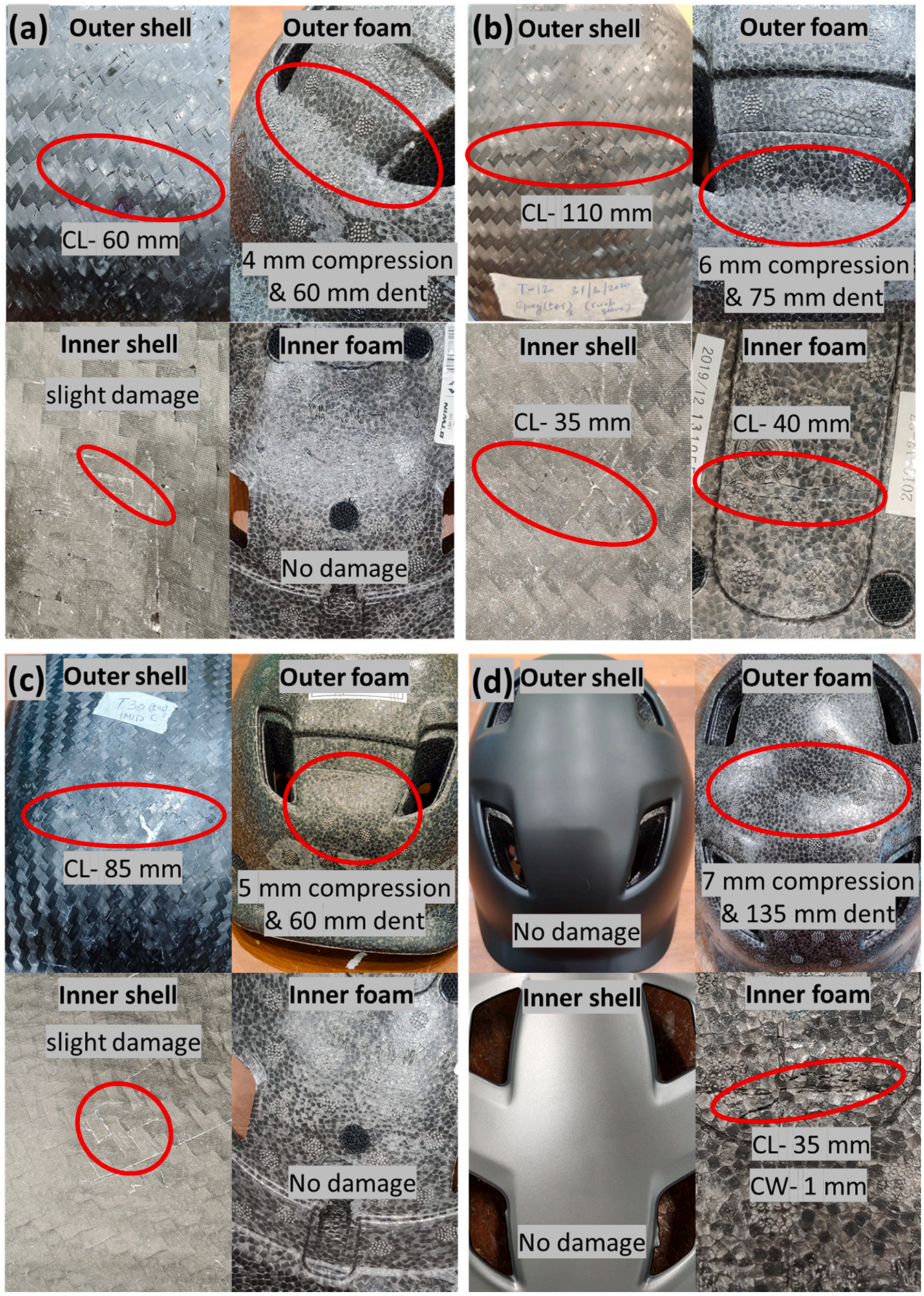

Fig. 9. Post impacted images of the inner and outer side of the foams and shells impacted on the curb-stone anvil (a) CEL/EPS (b) CEP/EPS (c) CEL IM/EPS (d) PC/EPS configurations.

29,36,43]. Due to the extended plasticity and spread failure behaviour of the acrylic Elium® resin, the amount of load transferred to the foam is distributed over the area and as a result, the cracks in the foam are less severe in CEL/EPS configuration.

When the composite shell is compared to the PC/EPS configuration (refer Fig. 11d), it can be observed that the damage in the foam is much severe. Multiple cracks on the inner side of the foam can be observed with a crack length of about 80 mm and a crack wide opening of about 1.3 mm, which is comparatively more severe than the composite shell variants. The reason for this is directly related to the previous explanation that for PC/EPS configuration as the maximum load is taken by the foam and the total energy absorbed by the foam in the terms of crack or deformation (78.5% out of total 86.3% absorbed energy). The inner foam crack delivers a very good understanding of the importance/effect of the material system in terms of safety it is in direct contact with the human head. Thus, concerning safety concerns, composite helmets are much safer than the PC/EPS helmet. Also, from the failure mechanism, it is very evident that the thermoplastic Elium® and Elium®IM composite shell helmet is a better choice than the conventional Epoxy composite shell helmet. In the case of toughened Elium®, Elium® Acrylic resin filled with ABS increases the matrix ductility in Elium® resin and leads to more plastic deformation under impact [30]. By making Elium® more ductile, the ABS typically act to resist and bridges the cracks and shields the matrix from cracking. It is evident from the literature that the main damage mode for the ductile materials is through cavitation. The improved performance of Elium® and Elium®IM composite shells in terms of damage, energy absorption, and the failure mode is due to the inherent ductility in case Elium® and due to micelle cavitation in the

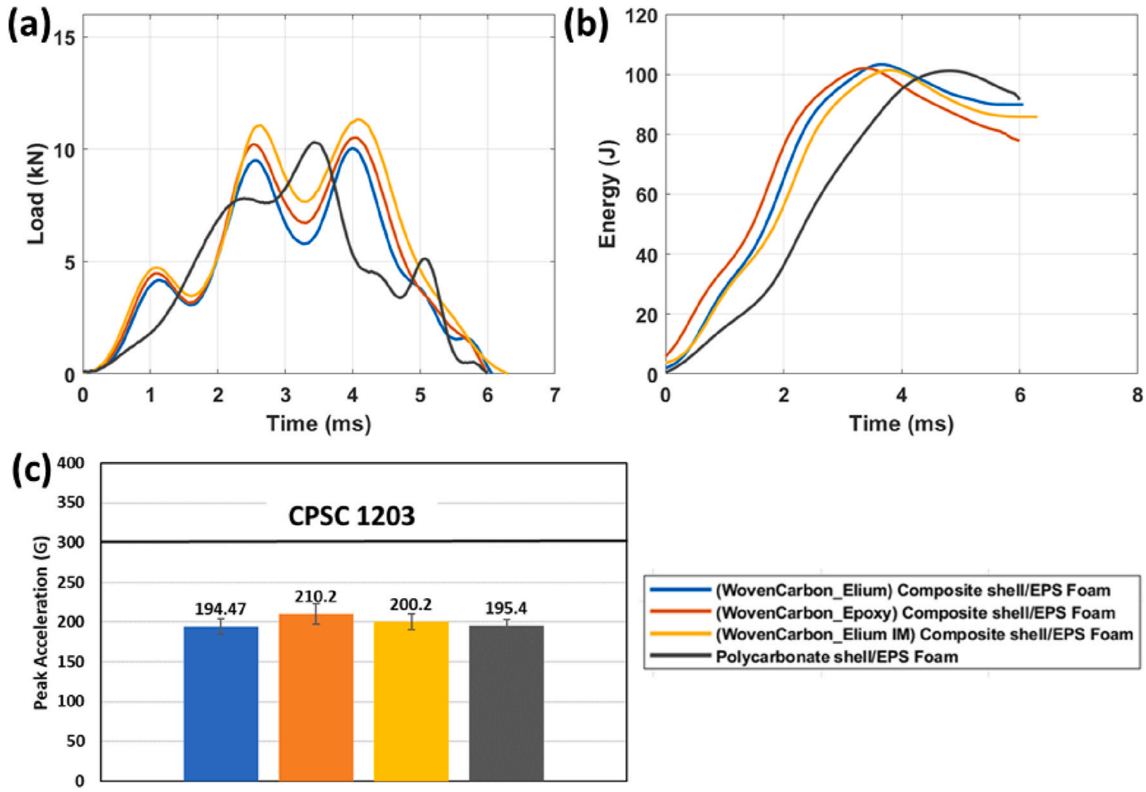

Fig. 10. (a) Load-time curve (b) Energy-time curve and (c) Peak acceleration for all the configurations impacted on the flat anvil.

Table 5
Calculated and Analyzed values for all helmet configurations impacted on the flat anvil.

Helmet configuration	CEL/EPS		CEP/EPS		CEL IM/EPS		PC/EPS	
Shell weight (g)	161		149		160.2		116	
Helmet weight (g)	271.1		258.4		267.5		230	
Impact	1st	2nd	1st	2nd	1st	2nd	1st	2nd
Peak Acceleration (G)	194.7 ± 9.5	197.2 ± 9.8	210.2 ± 11.3	213.8 ± 12.5	200.2 ± 9.86	198.5 ± 8.5	195.4 ± 7.85	198.2 ± 7.43
Peak Load (kN)	10.04 ± 0.27	11.42 ± 0.23	11.32 ± 0.26	12.08 ± 0.31	10.52 ± 0.32	9.12 ± 0.38	10.03 ± 0.28	11.15 ± 0.25
Impact energy E_{im}(J)	103.3	101.5	102.01	101.12	101.37	101.34	101.15	99.58
Absorbed energy at the end of impact event, E_{ab}(J)	89.9	90.4	77.86	78.4	85.8	84.2	90.5	87.65
E_{ab} (% of E_{im})	85.09	87.72	68.98	71.02	81.85	79.64	88.2	86.39
Contact time, $t_{contact}$ (ms)	6.06	6.23	5.99	5.78	6.3	6.21	6	5.82
HIC	1416	1390	1489	1498	1379	1373	1587	1592
Major energy absorbed by shell (%)	51.85	52.65	48.68	49.21	53.38	51.92	12.81	7.89
Major energy absorbed by foam (%)	35.62	37.35	25.17	22.92	28.47	27.72	75.39	78.5

case of Elium®IM which enhances the toughness of the matrix [22,25,28–30,43]. Under the drop impact, the cavitation phenomenon reduces severe deamination as in the case of brittle epoxy matrices and prevents delamination [43], and creates matrix shear banding [30,31].

4.3. Impact of carbon reinforcement helmet: hemispherical anvil

a Testing and data analysis

Fig. 12(a–b) represents Load-time and Energy-time curves for all the helmet configurations of first impact sites. Table 6 shows the analyzed results of both the impact sites on the hemispherical anvil. From Fig. 12, it can be depicted that for all the composite helmet configurations, the peak load and peak acceleration values are almost similar. All the helmet configurations pass the CPSC 1203 standard i.e. <300 G when impacted on the hemispherical anvil. The PC/EPS configuration (reference helmet) shows a much higher peak load compared to all the composite configurations and proportionally the peak acceleration is also much higher than the composite shell helmet. The peak acceleration of the PC/EPS configuration is 64.6%, 66%, and 63.2% higher compared to CEL/EPS, CEP/EPS, and CEL IM/EPS helmet configurations respectively.

Similar to the case of flat anvil impacts, CEL IM/EPS shows the highest contact time during the impact event (9.15 ms) followed by CEL/EPS (7.9 ms), and CEP/EPS (7.7 ms) configurations. PC/EPS configuration shows the least contact time of all configurations (7.35 ms). Also, while comparing the % energy absorption (refer Table 6), all the composite configurations have shown similar results and absorb the total impact energy. Whereas the % energy absorption in PC/EPS configurations is 84.4% of the total impacted energy. But the nature of energy absorptions by shells and foam are very different. The reason can be explained as in the composite shell helmets, the majority of the energy is absorbed by the shell whereas in the case of PC/EPS

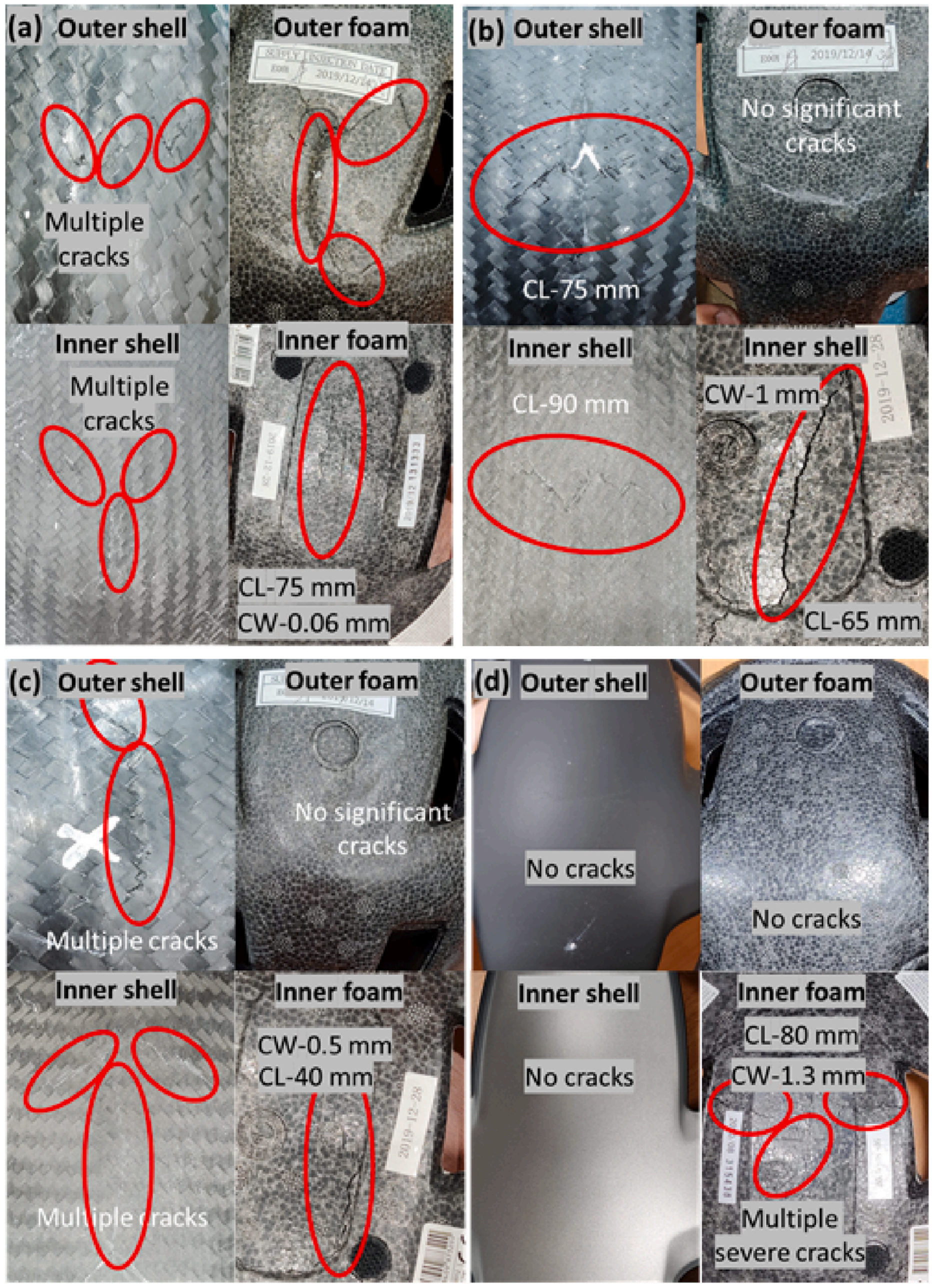

Fig. 11. Post impacted images of the inner and outer side of the foams and shells impacted on the flat anvil (a) CEL/EPS (b) CEP/EPS (c) CEL IM/EPS (d) PC/EPS configurations.

configuration maximum load is transferred to the foam and absorbed by the foam. As seen in Table 6, the HIC value of the PC/EPS configuration is almost 86% higher than the CEL/EPS configuration. All the configurations are below 700 HIC, so the fatality rate for all configurations is 0%. But the critical injury rate for PC/EPS (3%) is almost twice as compared to composite shell configuration (1.3%).

b. Damage analysis

From Fig. 13, it can be observed that for the helmet foam on the outer side, there is a huge dent/compression of the foam but there was no crack propagation on the inner side of the foam for all configurations. From Fig. 13a-c, the shell of the CEL/EPS and CEL IM/EPS configurations, it can be observed that damage for both the configurations is comparatively lesser and there is more spread out the failure of the cracks. Whereas in CEP/EPS configuration, it can be observed that the crack on the shell is more concentrated as in the case with the flat anvil, and also the crack length is relatively higher.

The wide-spread failure in the CEL configuration helmet helps to dissipate the energy and the amount of load transferred to the foam is also comparatively lesser. This can be observed from the compression of the foam and its diameter. CEP/EPS foam shows comparatively more compression of 7 mm and dent area of diameter 60 mm, as compared to the other composite shell configurations (5 mm compression and dent area of diameter 50 mm) due to the catastrophic failure of the shell. Similarly, while comparing the composite shell configurations to PC/EPS helmet (refer Fig. 13d), the amount of foam compression and its spread is much higher as the majority of the load is transferred to the foam and minimal load is taken by the shell (PC). This also resulted in the crack formation through the thickness direction and propagation to the inner foam with a crack length of 25 mm (refer Fig. 13d). On the other hand, there is no crack in the inner foam of all the composite shell

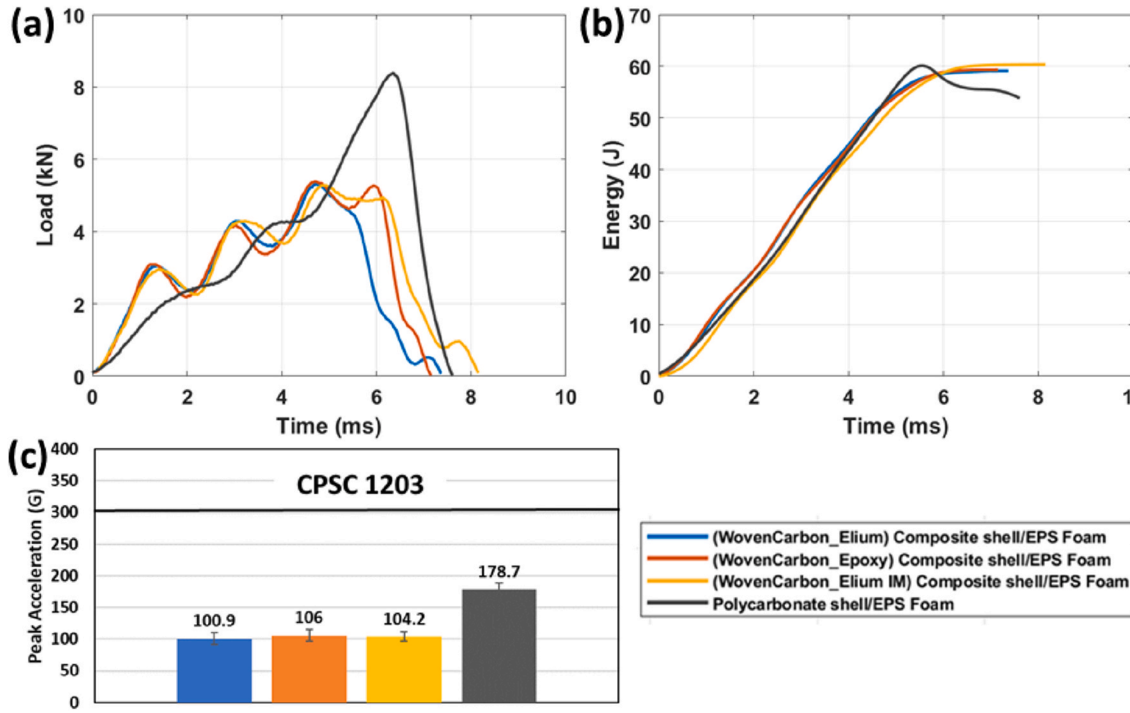

Fig. 12. (a) Load-time curve (b) Energy-time curve and (c) Peak acceleration for all the configurations impacted on the hemispherical anvil.

Table 6
Calculated and analyzed values for all helmet configurations impacted on Hemispherical anvil.

Helmet configuration	CEL/EPS		CEP/EPS		CEL IM/EPS		PC/EPS	
Shell weight (g)	161		149		160.2		116	
Helmet weight (g)	271.1		258.4		267.5		230	
Impact	1st	2nd	1st	2nd	1st	2nd	1st	2nd
Peak Acceleration (G)	100.9 ± 9.3	103.1 ± 8.9	106 ± 9.8	108.2 ± 9.3	104.2 ± 7.1	103 ± 9.7	178.7 ± 10.2	173 ± 7.6
Peak Load (kN)	5.26 ± 0.31	5.32 ± 0.23	5.8 ± 0.24	5.68 ± 0.29	5.26 ± 0.45	5.77 ± 0.41	8.38 ± 0.32	8.98 ± 0.42
Impact energy E_{im}(J)	58.57	59.11	60.17	59.34	59.7	60.35	60.11	57.81
Absorbed energy at the end of impact event, E_{ab}(J)	58.5	58.98	60.09	59.32	59.55	60.22	52.01	50.45
E_{ab} (% of E_{im})	99.88	99.78	99.87	99.97	99.70	99.78	84.43	85.41
Contact time, $t_{contact}$ (ms)	7.9	7.86	7.8	7.75	9.1	9.15	7.4	7.35
HIC	368	379	399	385	396	376	625	683
Major energy absorbed energy by shell (%)	42.34	41.14	36.29	37.23	43.92	43.21	9.23	11.11
Major energy absorbed energy by foam (%)	57.54	58.64	63.58	62.74	55.78	56.57	75.2	74.3

configurations. The benefit of the composite shell over the conventional PC shell can be observed in the form of energy absorption, crack formation, and damage propagation.

4.4. Head injury criteria: summary

If the HIC values are considered, the PC/EPS helmet performs least among all the configurations and the benefit of the composites over conventional helmets can be observed (refer Fig. 14). Among the composite helmets, a clear benefit of using Elium® and toughened Elium® resin system can be observed. For both the flat anvil, CEL/EPS and CEL IM/EPS composite helmet shows the fatality rate of 3% and 3.3% as opposed to 3.9% and 6% in case of CEP/EPS and PC/EPS respectively. Also with the manufactured Carbon/Elium® composite helmets, the chances of critical rates are reduced to 15% (CEL IM/EPS) while comparing with PC/EPS configuration (28.7%). For all the configurations tested on the curb-stone and hemispherical anvils, the fatality rate is 0% but CEL/EPS and CEL IM/EPS composite helmet shows critical injury rate reduced to 1.3% and 0.9% while comparing with conventional PC/EPS configuration with the critical injury rates of 2% and 3% for the respective anvils. Whereas, for curbstone anvil, carbon fibre composite helmet shows the best result.

5. Conclusions

Composite helmets with different types of matrix systems such as Elium®, Elium® IM, and Epoxy were successfully manufactured using a vacuum-assisted resin infusion process and they can be injected in as low as 1 min. All the helmet configurations were tested based on CPSC 1203 standard and accordingly were impacted on three different anvils Flat, Hemispherical, and Curbstone. The composite helmet configurations along with the PC/EPS helmet passed the CPSC peak acceleration criteria of below 300 G. Comparing the peak acceleration result among all the configurations, CEL/EPS showed the best result among all configurations. Considering the HIC value, the PC/EPS helmet showed the poorest result with a very high fatality rate on the flat anvil impact of 6% while the composite helmet can reduce the fatality rate to 3%. It was noticed that most of the energy absorption in the composite helmet was taken by the shell and helped in transferring less amount of load to the foam. On the other hand, for the PC/EPS helmet, the majority of the load was transferred to the foam which is not an ideal condition. The improved performance of Elium® and Elium® IM composite shells in terms of energy absorption and the failure mode is due to the inherent ductility in case Elium® and due to micelle cavitation in the case of Elium® IM which enhances the toughness of the matrix. Among the

Fig. 13. Post impacted images of the inner and outer side of the foams and shells impacted on the hemispherical anvil (a) CEL/EPS (b) CEP/EPS (c) CEL IM/EPS (d) PC/EPS configurations.

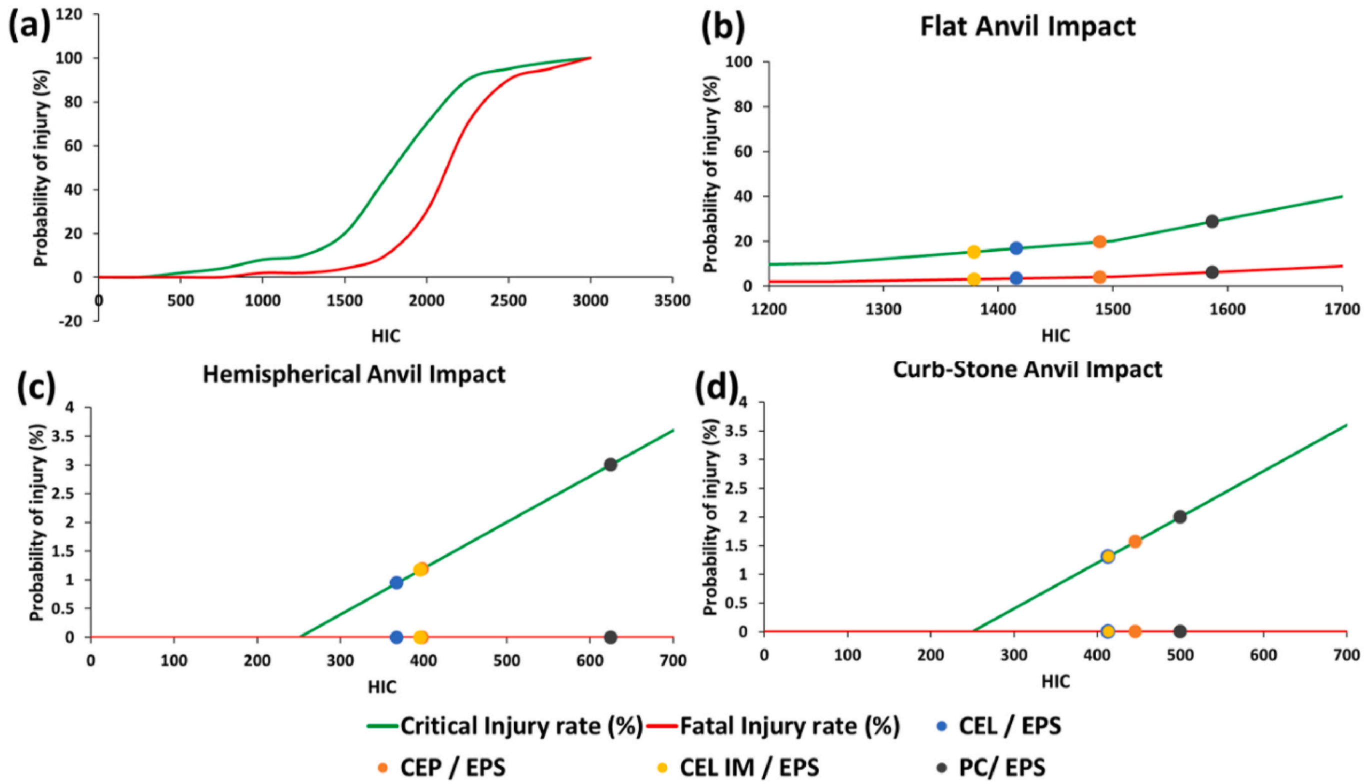

Fig. 14. HIC curves showing the probability of the critical injury and the fatality rate for different configurations of helmets (a) Typical HIC curve (b) Flat anvil (c) hemispherical anvil (d) curbstone anvil impact.

composite configurations, Elium® and Elium® infused composite shells showed a wide-spread failure and cracks were less severe. From the HSC analysis, a clear deformation of the composite shell was observed owing to the ductile behavior of the thermoplastic composite. On the other hand, Epoxy infused composite shells showed relatively more concentrated failure in a catastrophic manner. Overall, the detailed manufacturing and certification tests performed on the helmets have shown a significant potential of using carbon/Elium® composite shells as a viable alternative to the conventionally used material systems for helmets in terms of achieving enhanced safety.

Data availability

The raw data required to reproduce these findings cannot be shared at this time as the data also forms part of an ongoing study.

Declaration of competing interest

The authors declare that they have no known competing financial interests or personal relationships that could have appeared to influence the work reported in this paper.

Acknowledgments

The authors would like to acknowledge the financial support from Nanyang Technological University, Singapore, and Arkema, France for financial support under the RCA18/46. This research is supported by A*STAR under the Research Innovation Enterprise (RIE) 2020 Plan, Advanced Manufacturing and Engineering (AME) Domain – Industry Alignment Fund – Pre-positioning (IAF-PP) Polymer Matrix Composites Programme, Grant number A19C9a0044, Work Package 1–2.

References

[1] Mindell J, et al. 2414 - head injuries as a cause of road travel death in cyclists, pedestrians and drivers. Journal of Transport & Health 2018;9:S29.
[2] Nakayama DK, Gardner MJ, Rogers KD. Disability from bicycle-related injuries in children. J Trauma 1990;30(11):1390–4.
[3] Neacsu, V., et al., Pultrusion and Resin film infusion (RFI) of bi-angle thin ply NCF, in JEC Composites Magazine. p. vol. 68:59-61.
[4] Hansen K, Engesaeter L, Viste A. Protective effect of different types of bicycle helmets. Traffic Inj Prev 2004;4:285–90.
[5] Di Landro L, Sala G, Olivieri D. Deformation mechanisms and energy absorption of polystyrene foams for protective helmets. Polym Test 2002;21(2):217–28.
[6] Miltz J, Ramon O. Energy absorption characteristics of polymeric foams used as cushioning materials. Polym Eng Sci 1990;30(2):129–33.
[7] Pinnoji PK, Mahajan P. Analysis of impact-induced damage and delamination in the composite shell of a helmet. Mater Des 2010;31(8):3716–23.
[8] Shuaeib FM, et al. Motorcycle helmet: Part II. Materials and design issues. J Mater Process Technol 2002;123(3):422–31.
[9] Gale AM, J N. Effect of polystyrene foam liner density on motorcycle helmet shock absorption. Plast Rubber Process Appl 1985;5(2):101–8.
[10] Gilchrist A, Mills NJ. Modelling of the impact response of motorcycle helmets. Int J Impact Eng 1994;15(3):201–18.
[11] Fernandes FAO, Alves de Sousa RJ. Motorcycle helmets—a state of the art review. Accid Anal Prev 2013;56:1–21.
[12] Bhudolia SK, et al. Effect of fixation stitches on out-of-plane response of textile non-crimp fabric composites. J Ind Textil 2018;48(7):1151–66. https://doi.org/10.1177/1528083718757525.
[13] Bhudolia SK, et al. Energy characteristics and failure mechanisms for textile spread tow thin ply thermoplastic composites under low-velocity impact. Fibers Polym 2019;20(8):1716–25.
[14] Kostopoulos V, et al. Finite element analysis of impact damage response of composite motorcycle safety helmets. Compos B Eng 2002;33(2):99–107.
[15] Cernicchi A, Galvanetto U, Iannucci L. Virtual modelling of safety helmets: practical problems. International Journal of Crashworthiness - INT J CRASHWORTHINESS 2008;13:451–67.
[16] Denneulin S, Philippe V. Behavior of composite and polycarbonate plate under impact. 6, http://doi.org/10.1051/epjconf/20100615005; 2010.
[17] Vishal Shinde, A.D., Subir Khan, Design and analysis of indusrtial safety helmet using composite material. IOSR journal of mechanical and civil engineering (IOSR-JMCE)..
[18] B RM. Design and FE analysis of hybrid composite motorcycle helmet. Int. J. Innov. Res. Adv. Eng. (IJIRAE) 2018;5(1).
[19] Bhudolia SK, Perrotey P, Joshi SC. Optimizing polymer infusion process for thin ply textile composites with novel matrix system. Materials 2017;10(3).

[20] van Rijswijk K, Bersee HEN. Reactive processing of textile fiber-reinforced thermoplastic composites – an overview. Compos Appl Sci Manuf 2007;38(3):666–81.
[21] Bhudolia SK, Perrotey P, Joshi SC. Mode I fracture toughness and fractographic investigation of carbon fibre composites with liquid Methylmethacrylate thermoplastic matrix. Compos B Eng 2018;134(Supplement C):246–53.
[22] Bhudolia SK, Joshi SC. Low-velocity impact response of carbon fibre composites with novel liquid Methylmethacrylate thermoplastic matrix. Compos Struct 2018;203:696–708.
[23] Bhudolia SK, Perrotey P, Joshi SC. Optimizing polymer infusion process for thin ply textile composites with novel matrix system. Materials 2017;10(3):293.
24 Barbosa LCM, Bortoluzzi DB, Ancelotti AC. Analysis of fracture toughness in mode II and fractographic study of composites based on Elium® 150 thermoplastic matrix. Composites Part B: Engineering 2019;175:107082.
[25] Shanmugam L, et al. Enhanced mode I fracture toughness of UHMWPE fabric/thermoplastic laminates with combined surface treatments of polydopamine and functionalized carbon nanotubes. Compos B Eng 2019:107450.
[26] Bhudolia SK, Perrotey P, Joshi SC. Experimental investigation on suitability of carbon fibre thin plies for racquets. Proc Inst Mech Eng P J Sports Eng Technol 2015;230(2):64–72. https://doi.org/10.1177/1754337115598489.
[27] Taillemite S. Arkema gains ground in composites and launches a revolutionary range of Elium liquid resins. 2014 03/03/2014. Available from: http://www.arkema.com/en/media/news/news-details/Arkema-gains-ground-in-composites-and-launches-a-revolutionary-range-of-Elium-liquid-resins/. [Accessed 12 February 2017].
[28] Matadi Boumbimba R, et al. Glass fibres reinforced acrylic thermoplastic resin-based tri-block copolymers composites: low velocity impact response at various temperatures. Compos Struct 2017;160:939–51.
[29] Obande W, Ray D, Ó Brádaigh CM. Viscoelastic and drop-weight impact properties of an acrylic-matrix composite and a conventional thermoset composite – a comparative study. Mater Lett 2019;238:38–41.
[30] Kinvi-Dossou G, et al. Innovative acrylic thermoplastic composites versus conventional composites: improving the impact performances. Compos Struct 2019;217:1–13.
[31] Shah SZH, et al. Performance comparison of resin-infused thermoplastic and thermoset 3D fabric composites under impact loading. Int J Mech Sci 2021;189:105984.
[32] Bhudolia SK, Perrotey P, Joshi SC. Enhanced Vibration damping and dynamic mechanical characteristics of composites with novel pseudo-thermoset matrix system. Composite Structures; 2017.
[33] Bhudolia SK, Perrotey P, Joshi SC. Enhanced vibration damping and dynamic mechanical characteristics of composites with novel pseudo-thermoset matrix system. Compos Struct 2017;179:502–13.
[34] Bhudolia SK, Perrotey P, Joshi SC. Experimental investigation on suitability of carbon fibre thin plies for racquets. Proc Inst Mech Eng P J Sports Eng Technol 2015. 1754337115598489.
[35] Bhudolia SK, et al. Flexural characteristics of novel carbon methylmethacrylate composites. Composites Communications 2019;13:129–33.
36 Kazemi ME, et al. Mechanical properties and failure modes of hybrid fiber reinforced polymer composites with a novel liquid thermoplastic resin. *Elium*®. Composites Part A: Applied Science and Manufacturing 2019;125:105523.
[37] Bhudolia SK, Joshi SC, Boon YD. Experimental and microscopic investigation on mechanical performance of textile spread-tow thin ply composites. Fibers Polym 2019;20(5):1036–45.
38 Bhudolia S·K, et al. Fatigue response of ultrasonically welded carbon/Elium® thermoplastic composites. Materials Letters 2020;264:127362.
39 Bhudolia S·K, et al. Ultrasonic Welding of Novel Carbon/ Elium® Thermoplastic Composites with Flat and Integrated Energy Directors: Lap Shear Characterization and Fractographic Investigation. Materials 2020;13(7):1634.
40 Bhudolia S·K, et al. Investigation on Ultrasonic Welding Attributes of Novel Carbon/Elium® Composites. Materials 2020;13(5):1117.
[41] Murray RE, Roadman J, Beach R. Fusion joining of thermoplastic composite wind turbine blades: Lap-shear bond characterization. Renew Energy 2019;140:501–12.
[42] Manikandan P, Chai GB. A similitude approach towards the understanding of low velocity impact characteristics of bi-layered hybrid composite structures. Compos Struct 2015;131:183–92.
[43] Bhudolia S·K, et al. Damping, impact and flexural performance of novel carbon/Elium® thermoplastic tubular composites. Composites Part B: Engineering 2020;203:108480.
[44] Newman JA. Head injury criteria in automotive crash testing. 1980. p. 47.
[45] Ono K, Kikuchi A, Nakamura M, Kobayashi H, et al. Human head tolerance to sagittal impact reliable estimation deduced from experimental head injury using subhuman primates and human cadaver skulls. SAE Technical Paper 1980:801303. https://doi.org/10.4271/801303.
[46] Nikmatin S, et al. Evaluation of the performance of helmet prototypes fabricated from acrylonitrile butadiene styrene composites filled with natural resource. Materials 2019;12(1):34.
[47] Bhudolia S·K, et al. Quasi-static indentation response of core-shell particle reinforced novel NCCF/Elium® composites at different feed rates. Composites Communications 2020;21:100383.
[48] Offringa AR. Thermoplastic composites—rapid processing applications. Compos Appl Sci Manuf 1996;27(4):329–36.
[49] Garesci F, Fliegener S. Young's modulus prediction of long fiber reinforced thermoplastics. Compos Sci Technol 2013;85:142–7.
[50] Zhang D, et al. Out of autoclave consolidation of voids in continuous fiber reinforced thermoplastic composites. In: SAMPE 2013 conference and exhibition: education and green sky - materials technology for a better world; 2013. Long Beach, CA.
[51] Lessard H, Lebrun G, Pham XT. Experimental evaluation of the thermo-stamping process for a 3D composite part made of unidirectional CF/PEEK prepregs. In: SAMPE tech 2013 conference and exhibition. Wichita, KS: Soc. for the Advancement of Material and Process Engineering; 2013.
[52] Vijendra B, Sharma A. Induction heated tool assisted friction-stir welding (i-FSW): a novel hybrid process for joining of thermoplastics. J Manuf Process 2015;20:234–44.
[53] Ning H, et al. Design and manufacturing of long fiber thermoplastic composite helmet insert. Compos Struct 2017;168:792–7.